

Evaluation of Losses in Pedestal-Supported Finlines

B. Gupta and S. Sural Majumdar
Jadavpur University, Calcutta - 700 032.

ABSTRACT

A technique for evaluation of conductor and dielectric losses in pedestal-supported finlines using mixed spectral domain approach has been presented. All field components were computed through application of Galerkin's technique in spectral domain, assuming weighted basis functions to represent unknown electric voltages, i.e., magnetic currents. In the process, the propagation constant along the line was also accurately computed. The aim was to study attenuation behaviour of these lines wrt variation in dimensional and other structural parameters. The results indicated a specific dimensional range within which their use is justifiable. The potential defence applications of pedestal-supported finlines is in millimeter wave systems, e.g., radars, missile guidance systems, etc.

NOMENCLATURE

L_d	Dielectric loss
L_c	Conduction loss
ω	Angular frequency
ϵ	Permittivity of the dielectric
$\tan \delta$	Loss tangent of the dielectric
S_d	Cross-sectional area of the dielectric
R_s	Surface resistance
C	Total conductor periphery
\vec{H}_t	Tangential magnetic field over the conductor surface
\vec{E}_0, \vec{H}_0	Electric and magnetic fields, respectively in the cross-sectional plane

1. INTRODUCTION

For frequencies at the lower end of the millimeter wave (MMW) spectrum, finline offers a versatile transmission medium¹, which contains

metallic fins on one or both sides of a dielectric slab suspended within a rectangular conducting enclosure. The dielectric substrate has to be supported either by grooves or pedestals. With comparable dielectric and channel dimensions, a pedestal-supported quasi-planar transmission line enjoys advantages, such as larger bandwidth, wider impedance range and less sensitivity of impedance to dimensional tolerances over groove-supported structures^{2,3}. The cross-sectional view of a pedestal-supported bilateral finline is presented in Fig. 1.

The available literature does not provide proper account of losses for wave propagation along a pedestal-supported finline, although transmission loss should be considered a very important criterion while evaluating the performance of a transmission line. Hence, a method of loss evaluation in pedestal-supported

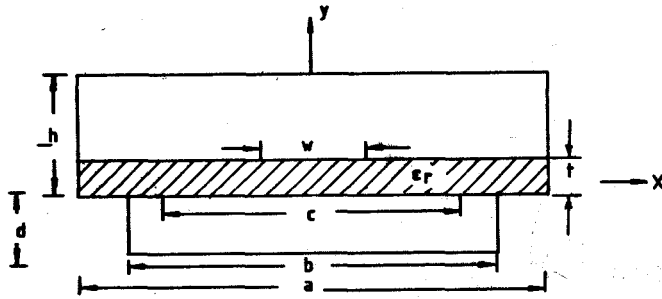


Figure 1. Cross-section of pedestal-supported bilateral finline

finlines using mixed spectral domain approach has been devised. Novelty of the work lies in the evaluation of losses considering the effect of pedestal, which has not been reported in the literature so far.

Today, electronic warfare is heavily dependent on MMW circuits and systems. MMW systems used for defence applications, viz., radars, missile guidance systems, etc. have to incorporate quasi-planar transmission structures like finlines, image dielectric guides, etc. Of these, either groove-supported or pedestal-supported finlines are preferred for certain applications. Since the pedestal-supported finlines are superior in performance to groove-supported finlines for reasons stated above and since their total losses considering the presence of pedestal also are presented for the first time here, this study will be extremely useful in designing MMW finline-based defence electronic systems. The results presented here establish a proper dimensional range of such lines which would ensure low-loss performance, which is always a prime design concern for obvious reasons.

2. THEORETICAL BACKGROUND

In the spectral domain approach, Galerkin's method is used in the Fourier transform domain to get a homogeneous system of equations for determining the unknown propagation constant and relative amplitudes of current distribution along a planar or quasi-planar transmission line. The Fourier transform is taken along a direction parallel

to the substrate and perpendicular to the direction of propagation. The transform is defined by

$$\tilde{\Phi}(\alpha) = \int_{-\infty}^{\infty} \phi(x) e^{j\alpha x} dx \quad (1)$$

where α is a discrete Fourier variable.

Since the regions above and below the pedestal support have different sidewall separations, it requires mixing of the two different spectral domains (which exist on two sides of the pedestal support) to investigate the structure.

For the pedestal-supported finline shown in Fig. 1, the aperture at $y = t$ plane is replaced by a perfectly conducting plane (shorted aperture) with the original tangential electric field at the aperture restored at $y = t+$ and $y = t-$ by appropriate magnetic

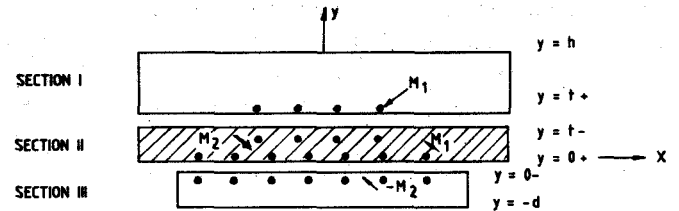


Figure 2. Equivalent structure used for analysis

surface currents M_1 and $-M_1$, respectively. Similarly, the aperture at $y = 0$ plane is replaced by a perfectly conducting plane and appropriate magnetic surface currents M_2 and $-M_2$. The resulting equivalent structure is shown in Fig. 2.

The hybrid fields in each of the three regions in Fig. 2 are first expressed in terms of superposition of *TE*-to-*y* and *TM*-to-*y* expressions involving scalar potentials. The transverse magnetic fields in the spectral domain at the planes $y = t$ and $y = 0$ approaching from either side of each plane may be obtained in terms of unknown magnetic currents and spectral domain Green's functions as

$$\begin{bmatrix} \tilde{H}_x \\ \tilde{H}_z \end{bmatrix}_{t\pm} = \begin{bmatrix} \tilde{G}_{xx}^1 & \tilde{G}_{xz}^1 \\ \tilde{G}_{zx}^1 & \tilde{G}_{zz}^1 \end{bmatrix} \begin{bmatrix} \tilde{M}_{1x} \\ \tilde{M}_{1z} \end{bmatrix} \quad (2)$$

$$\begin{bmatrix} \tilde{H}_x \\ \tilde{H}_z \end{bmatrix}_{t-} = \begin{bmatrix} \tilde{G}_{xx}^2 & \tilde{G}_{xz}^2 \\ \tilde{G}_{zx}^2 & \tilde{G}_{zz}^2 \end{bmatrix} \begin{bmatrix} \tilde{M}_{1x} \\ \tilde{M}_{1z} \end{bmatrix} + \begin{bmatrix} \tilde{G}_{xx}^3 & \tilde{G}_{xz}^3 \\ \tilde{G}_{zx}^3 & \tilde{G}_{zz}^3 \end{bmatrix} \begin{bmatrix} \tilde{M}_{2x} \\ \tilde{M}_{2z} \end{bmatrix} \quad (3)$$

$$\begin{bmatrix} \tilde{H}_x \\ \tilde{H}_z \end{bmatrix}_{o+} = \begin{bmatrix} \tilde{G}_{xx}^4 & \tilde{G}_{xz}^4 \\ \tilde{G}_{zx}^4 & \tilde{G}_{zz}^4 \end{bmatrix} \begin{bmatrix} \tilde{M}_{1x} \\ \tilde{M}_{1z} \end{bmatrix} + \begin{bmatrix} \tilde{G}_{xx}^5 & \tilde{G}_{xz}^5 \\ \tilde{G}_{zx}^5 & \tilde{G}_{zz}^5 \end{bmatrix} \begin{bmatrix} \tilde{M}_{2x} \\ \tilde{M}_{2z} \end{bmatrix} \quad (4)$$

$$\begin{bmatrix} \tilde{H}_x \\ \tilde{H}_z \end{bmatrix}_{o-} = \begin{bmatrix} \tilde{G}_{xx}^6 & \tilde{G}_{xz}^6 \\ \tilde{G}_{zx}^6 & \tilde{G}_{zz}^6 \end{bmatrix} \begin{bmatrix} \tilde{M}_{2x} \\ \tilde{M}_{2z} \end{bmatrix} \quad (5)$$

Here, quantities with tilde (\sim) represent Fourier transforms of corresponding spatial domain quantities, while x or z in the subscript refers to the corresponding direction. Enforcing continuity of transverse magnetic field across the apertures at $y = t$ and $y = 0$ in the spatial domain, one gets

$$\begin{bmatrix} H_x \\ H_z \end{bmatrix}_{t-} = \begin{bmatrix} H_x \\ H_z \end{bmatrix}_{t+} \quad (6a)$$

and

$$\begin{bmatrix} H_x \\ H_z \end{bmatrix}_{o-} = \begin{bmatrix} H_x \\ H_z \end{bmatrix}_{o+} \quad (6b)$$

However, it is to be noted that one should be careful in applying Eqns 6(a) and 6(b) to the spectral domain when different quantities are to be replaced by their Fourier transforms, due to the fact that different spectral domains having different spectral variables exist at $y = 0+$ and $y = 0-$ planes.

To solve for unknown magnetic currents using spectral domain immittance approach, first, the unknown magnetic currents are expanded in terms of known basis functions with unknown amplitude factors as

$$M_{1x} = \sum_{i=1}^P c_{1xi} m_{1xi}(x, w/2)$$

$$M_{1z} = \sum_{i=1}^P c_{1zi} m_{1zi}(x, w/2)$$

$$M_{2x} = \sum_{i=1}^Q c_{2xi} m_{2xi}(x, c/2)$$

$$M_{2z} = \sum_{i=1}^Q c_{2zi} m_{2zi}(x, c/2)$$

Taking inner products of the spatial domain Eqns 6(a) and (6b) wrt M_{1xi} ($i = 1, \dots, P$), M_{1zi} ($i = 1, \dots, P$), M_{2xi} ($i = 1, \dots, Q$) and M_{2zi} ($i = 1, \dots, Q$), respectively and applying Parseval's theorem, one gets a matrix equation of the form

$$[A][X] = 0 \quad (7)$$

where $[X]$ is a vector composed by the unknown magnetic current weighting factors. The coefficient matrix $[A]$ may be written in terms of sub-matrices as

$$[A] = \begin{bmatrix} [S_{11}]_{PXP} & [S_{12}]_{PXP} & [S_{13}]_{PXQ} & [S_{14}]_{PXQ} \\ [S_{21}]_{PXP} & [S_{22}]_{PXP} & [S_{23}]_{PXQ} & [S_{24}]_{PXQ} \\ [S_{31}]_{QXP} & [S_{32}]_{QXP} & [S_{33}]_{QXQ} & [S_{34}]_{QXQ} \\ [S_{41}]_{QXP} & [S_{42}]_{QXP} & [S_{43}]_{QXQ} & [S_{44}]_{QXQ} \end{bmatrix} \quad (8)$$

A typical sub-matrix element will be of the form

$$S_{33}(i, k) = \sum_{n=-\infty}^{\infty} \left[\frac{1}{a} \left\{ \tilde{M}_{2xi} \tilde{G}_{xx}^5 \tilde{M}_{2xk} \right\}_{\alpha_a} - \frac{1}{b} \left\{ \tilde{M}_{2xi} \tilde{G}_{xx}^6 \tilde{M}_{2xk} \right\}_{\alpha_b} \right] \quad (9)$$

The discrete Fourier transform variables to be chosen are $\alpha_a = 2n\pi/a$ for region with sidewall separation a and $\alpha_b = 2n\pi/b$ region with sidewall separation b . Expressions obtained for the spectral domain Green's functions are given in the Appendix 1.

3. DETERMINATION OF PROPAGATION CONSTANT

Matrix Eqn (4) forms a set of homogeneous equations in unknown magnetic current basis

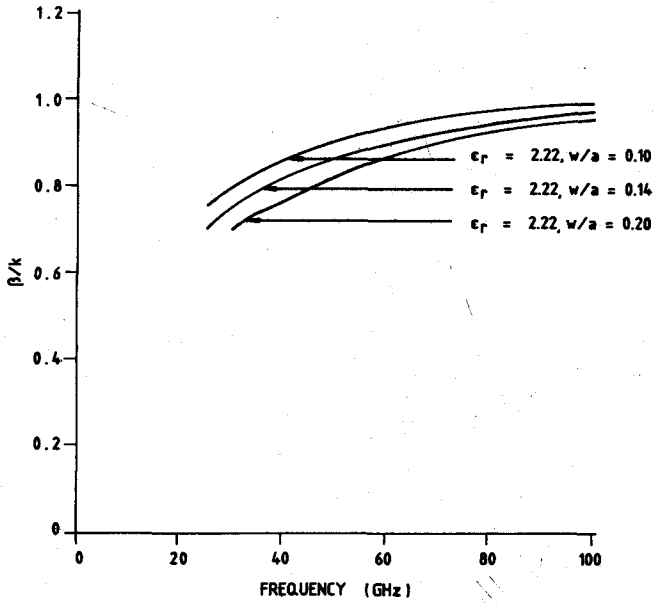


Figure 3. Propagation constant vs frequency for various values of w/a .

function amplitudes which will have a nontrivial solution set provided the coefficient matrix $[A]$ has got zero determinant. Since all the terms in $[A]$ implicitly contain the constant β , setting its determinant to zero and adopting a root-searching technique using the modified secant method, one can solve β .

Inner product of two functions $f(x)$ and $g(x)$ in a region having width L along x -direction is given by

$$\int_{-L/2}^{L/2} f(x)g(x)dx$$

which may be replaced by $\frac{1}{L} \sum_{n=-\infty}^{\infty} \tilde{f}(\alpha) \tilde{g}(\alpha)$ i.e., an infinite summation over a discrete spectral variable α by application of Parseval's theorem.

4. DETERMINATION OF LOSSES

Once the propagation constant is evaluated, the fields in all regions can be obtained after solving the unknown magnetic current weighting coefficients.

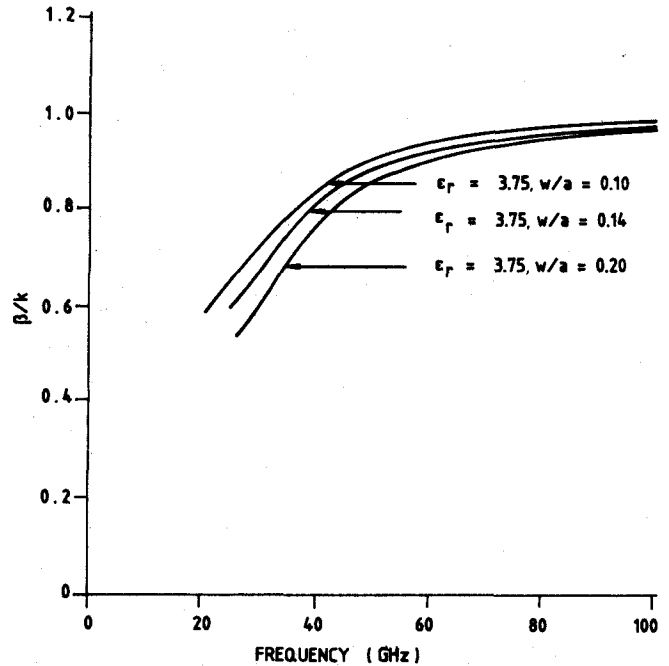


Figure 4. Propagation constant vs frequency for various values of w/a .

Thus, knowing all field expressions, losses were computed⁴ as

$$L_d = \frac{\omega \epsilon \tan \delta \int_{s_d} |\vec{E}_0|^2 ds}{2 \text{Re} \int_s \vec{E}_0 \times \vec{H}_0^* \cdot d\vec{s}} Np/m$$

and

$$L_c = \frac{R_s \int_{s_d} |H_t|^2 dl}{2 \text{Re} \int_s \vec{E}_0 \times \vec{H}_0^* \cdot d\vec{s}} Np/m$$

5. CHOICE OF BASIS FUNCTIONS

The basis functions are to be chosen to represent the magnetic currents, i.e., electric voltages across the slots accurately, taking into consideration proper edge corrections. The basis functions chosen were:

$$M_{xi}(x, \rho) = (-1)^i \frac{\sin[2i\pi x / \rho]}{\sqrt{1 - (2x/\rho)^2}}$$

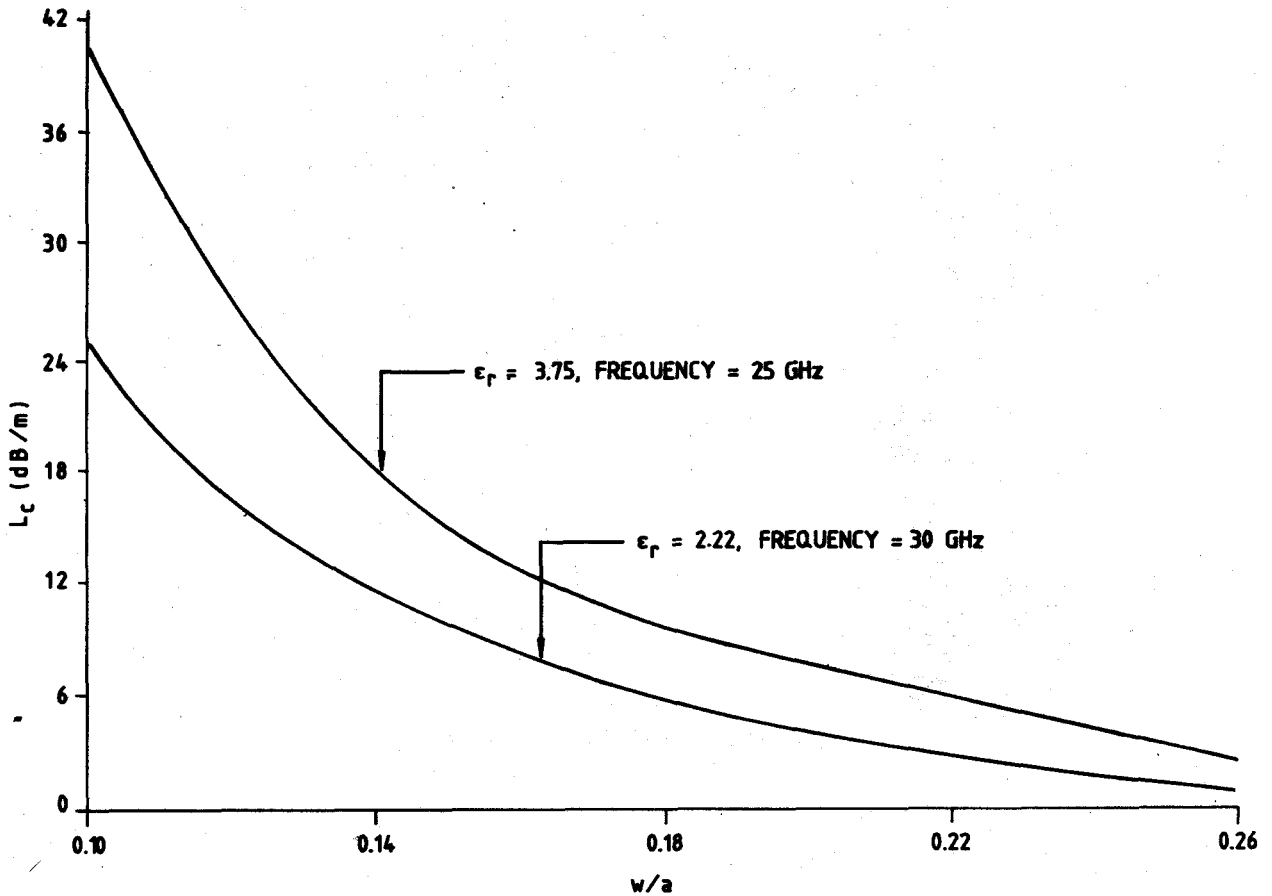


Figure 5. Conduction loss vs slot width

$$M_{zi}(x, \rho) = (-1)^{i-1} \frac{\cos[2(i-1)\pi x / \rho]}{\sqrt{1-(2x/\rho)^2}}$$

for an x-directed slot of width ρ .

These functions were chosen noting the inherent symmetry of the structure. They are analytically transformable to yield the following transforms:

$$\tilde{M}_{zi}(\alpha, \rho) = (-1)^i \frac{\pi \rho}{4j} \left[\left(J_0 \left| \frac{\alpha \rho}{2} + i\pi \right| \right) - J_0 \left(\left| \frac{\alpha \rho}{2} - i\pi \right| \right) \right]$$

and

$$\tilde{M}_{zi}(\alpha, \rho) = (-1)^{i-1} \frac{\pi \rho}{4} \left[\left(J_0 \left| \frac{\alpha \rho}{2} + (1-i)\pi \right| \right) - J_0 \left(\left| \frac{\alpha \rho}{2} - (i-1)\pi \right| \right) \right]$$

The number of basis functions required were determined after proper convergence test for various slot widths and the number used varied from 1 to 3.

6. CHECKING FOR ACCURACY

For checking accuracy of the results, few data points were chosen from Figs 2 and 3 of Ref. 4. They represent propagation constant, and loss computation results for unilateral finlines; a limiting case of pedestal-supported finlines obtained by setting $a = b = c$ in the geometry

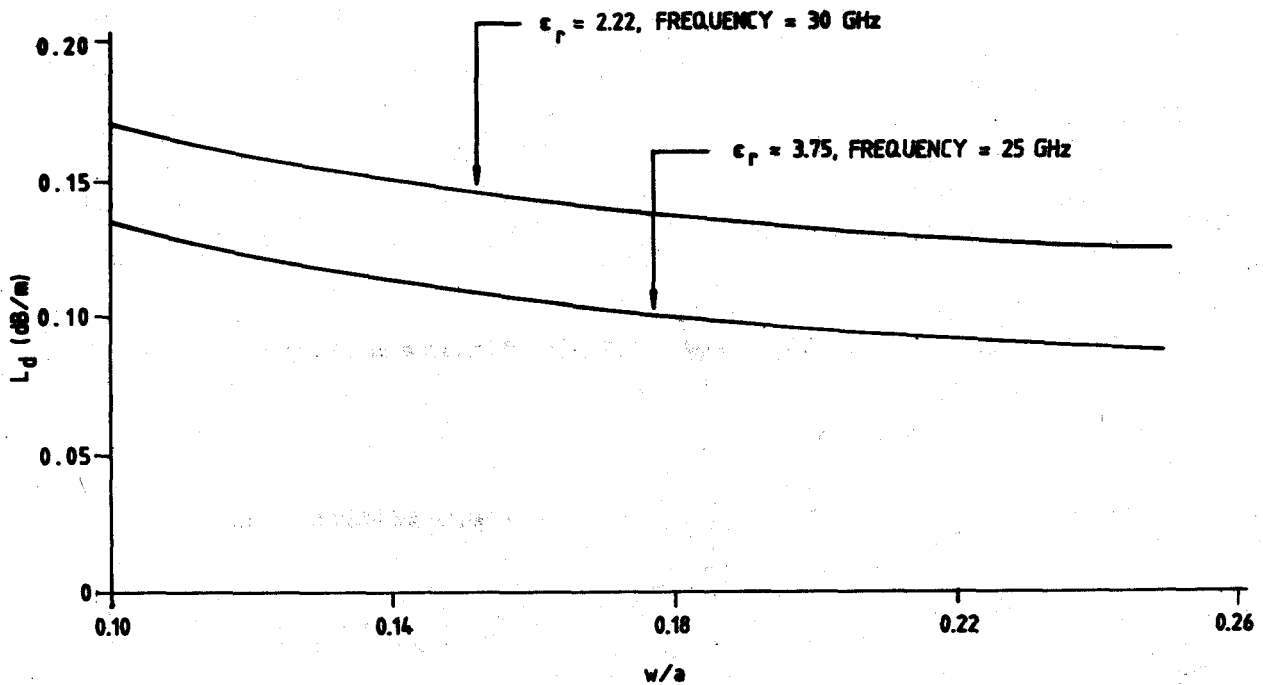


Figure 6. Dielectric loss vs slot width

(Fig. 1). Results thus obtained for the same set of parameters agreed with the results presented in Ref. 4 are given in Table 1.

7. COMPUTED RESULTS

Figures 3 and 4 show the dispersion characteristics, i.e., variation of normalised propagation constant with frequency for different sets of parameters. Figures 5 and 6 show variations of both L_c and L_d against normalised slot width for two different sets of parameters. For all graphs presented, the following data (wrt Fig. 1) were assumed:

$h = 3.6185 \text{ mm}, t = 0.1250 \text{ mm}$
 $d = 3.4925 \text{ mm}, a = 3.5560 \text{ mm}$

and $b = 1.7780 \text{ mm}, \tan \delta = 2 \times 10^{-4}$

$\sigma = 5.8 \times 10^{-7} \text{ mho/m.}$

It is further assumed that $c = w$, i.e., a symmetric bilateral finline structure R_s , i.e., surface resistance of conductor was computed using its standard expression⁵.

Based on the observations of these and other such curves (not presented here for the sake of brevity) it was found that the losses were within tolerable limits provided the normalised slot width exceeds a critical value of 0.2 or so. Also, as expected, the principal contribution to total losses is provided by the conductor loss and not by the dielectric loss.

Table 1. Propagation constant and loss computation results for unilateral finlines

Obs No.	Relative slot width (w/a)	Frequency (GHz)	Relative propagation constant (β/k_0)		Dielectric loss (dB/m)		Conductor loss (dB/m)	
			According to Ref. [4]	Computed	According to Ref. [4]	Computed	According to Ref. [4]	Computed
1	0.3	40	0.97295	0.9735	0.1555	0.1567	1.1667	1.1786
2	0.1	40	1.01700	1.0175	0.1778	0.1810	2.3332	2.3501
3	0.1	27	0.93750	0.9380	0.2556	0.2562	3.0000	3.0010

8. CONCLUSION

A new technique for exact computation of losses and their variations with frequency and slot width in a pedestal-supported bilateral finline has been proposed. The analysis is perfectly generalised and can be extended to unilateral or other finline structures with pedestal support after practically little or no modification. Moreover, considering applications of finlines to millimeter wave systems used in defence and electronic warfare, this study has great importance to Defence.

REFERENCES

1. Bhat, B. & Koul, S.K. Analysis, design and applications of finlines. Artech House Inc., 1987. pp. 1-30
2. Archer, J.W. An efficient 200-250 GHz frequency tripler incorporating a novel stripline structure. *IEEE Trans. Microw. Theory Tech.*, 1984, **MTT-32**, 416-20.
3. Chan, C.H.; Kwong, T. NG & Kouki, A.B. A mixed spectral domain approach for dispersion analysis of suspended planar transmission lines with pedestals. *IEEE Trans. Microw. Theory Tech.*, 1989, **MTT-37**, 1716-723.
4. Mirshekar Syahkal D. & Davies, J.B. An accurate, unified solution of various finline structures of phase constant, characteristic impedance and attenuation. *IEEE Trans. Microw. Theory Tech.*, 1982, **MTT-30**, 1854-861.
5. Jordan, E.C. & Balmain, K.G. Electromagnetic waves and radiating systems. Prentice Hall India Ltd., India, 1991. 155 p.

Contributors



Mr B Gupta obtained his ME (Telecom Engg) and PhD (Engg) both from the Jadavpur University, Calcutta, in 1984 and 1996, respectively. His research areas include computational electromagnetics, especially planar and quasi-planar circuits, including antennas and mathematical modelling. He is a senior member of the Institution of Engineers (India), IEEE, USA and a life member of Society of EMC Engineers (India). He is associated with a number of sponsored research projects and has published more than 18 research papers and also co-authored a book.

Ms S Sural Majumdar obtained her ME (Elect & Telecom Engg) from the Jadavpur University, Calcutta, in 1992 and 1995, respectively. Presently, she is working with CMC, Ltd. Her areas of research include software development in computer communication, microwave communication and software engineering.

Spectral Domain Green's Functions

$$\tilde{G}_{xx}^1(\alpha, \beta) = -y_{1h} N_x^2 - y_{1e} N_z^2$$

$$\tilde{G}_{xz}^1(\alpha, \beta) = \tilde{G}_{zx}^1(\alpha, \beta) = (y_{1e} - y_{1h}) N_x N_z$$

$$\tilde{G}_{zz}^1(\alpha, \beta) = -y_{1h} N_z^2 - y_{1e} N_x^2$$

$$\tilde{G}_{xx}^2(\alpha, \beta) = y_{2h} N_x^2 + y_{2e} N_z^2$$

$$\tilde{G}_{xz}^2(\alpha, \beta) = \tilde{G}_{zx}^2(\alpha, \beta) = (y_{2h} - y_{2e}) N_x N_z$$

$$\tilde{G}_{zz}^2(\alpha, \beta) = y_{2h} N_z^2 + y_{2e} N_x^2$$

$$\tilde{G}_{xx}^3(\alpha, \beta) = -y_{3h} N_x^2 - y_{3e} N_z^2$$

$$\tilde{G}_{xz}^3(\alpha, \beta) = \tilde{G}_{zx}^3(\alpha, \beta) = (y_{3e} - y_{3h}) N_x N_z$$

$$\tilde{G}_{zz}^3(\alpha, \beta) = -y_{3h} N_z^2 - y_{3e} N_x^2$$

$$\tilde{G}_{xx}^4(\alpha, \beta) = y_{4h} N_x^2 + y_{4e} N_z^2$$

$$\tilde{G}_{xz}^4(\alpha, \beta) = \tilde{G}_{zx}^4(\alpha, \beta) = (y_{4h} - y_{4e}) N_x N_z$$

$$\tilde{G}_{zz}^4(\alpha, \beta) = y_{4h} N_z^2 + y_{4e} N_x^2$$

$$\tilde{G}_{xx}^5(\alpha, \beta) = -y_{5h} N_x^2 - y_{5e} N_z^2$$

$$\tilde{G}_{xz}^5(\alpha, \beta) = \tilde{G}_{zx}^5(\alpha, \beta) = (y_{5e} - y_{5h}) N_x N_z$$

$$\tilde{G}_{zz}^5(\alpha, \beta) = -y_{5h} N_z^2 - y_{5e} N_x^2$$

$$\tilde{G}_{xx}^6(\alpha, \beta) = y_{6h} N_x^2 + y_{6e} N_z^2$$

$$\tilde{G}_{xz}^6(\alpha, \beta) = \tilde{G}_{zx}^6(\alpha, \beta) = (y_{6h} - y_{6e}) N_x N_z$$

$$\tilde{G}_{zz}^6(\alpha, \beta) = y_{6h} N_z^2 + y_{6e} N_x^2$$

$$y_{1e} = -\frac{j\omega\epsilon_0}{\gamma_1} \coth \gamma_1 (h-t), \quad y_{1h} = -\frac{\gamma_1}{j\omega\mu_0} \coth \gamma_1 (h-t)$$

$$y_{2e} = -\frac{j\omega\epsilon_0\epsilon_r}{\gamma_2} \coth \gamma_2 (h-t), \quad y_{2h} = -\frac{\gamma_2}{j\omega\mu_0} \coth \gamma_2 (h-t)$$

$$y_{3e} = -\frac{j\omega\epsilon_0\epsilon_r}{\gamma_2 \sinh \gamma_2 t}, \quad y_{3h} = -\frac{\gamma_2}{j\omega\mu_0 \sinh \gamma_2 t}$$

$$y_{4e} = y_{3e}, \quad y_{4h} = y_{3h}$$

$$y_{5e} = y_{2e}, \quad y_{5h} = y_{2h}$$

$$y_{6e} = -\frac{j\omega\epsilon_0}{\gamma_3} \coth \gamma_3 d, \quad y_{6h} = -\frac{\gamma_3}{j\omega\mu_0} \coth \gamma_3 d$$

$$N_x = \frac{\alpha}{\sqrt{\alpha^2 + \beta^2}}, \quad N_z = \frac{\beta}{\sqrt{\alpha^2 + \beta^2}}$$

$$\gamma_1 = \sqrt{\alpha^2 + \beta^2 - k^2} \quad \text{in Section } i$$

Obviously, α is to be defined separately for different regions as discussed.